Title

Monitoring Human Activity at a Very Local Scale with Ground-Motion Records: The Early Stage of COVID-19 Pandemic in California, U.S.A., New York City, U.S.A., and Mexicali, Mexico

Journal

Seismological Research Letters, 92(5)

ISSN

0895-0695

Authors

Wu, Baoning
Douilly, Roby
Ford, Heather A
et al.

Publication Date

2021-09-01

DOI

10.1785/0220200257

Peer reviewed

Monitoring human activity at a very local scale with ground motion records: the early stage of COVID-19 pandemic in California, USA, New York City, USA, and Mexicali, Mexico

Baoning Wu[1], Roby Douilly[1], Heather A. Ford[1], Gareth Funning[1], Hsin-Yu Lee[1], Shankho Niyogi[1], Manuel Mendoza[1], Christodoulos Kyriakopoulos[2,1], and David Oglesby[1]

[1]Department of Earth and Planetary Sciences, University of California, Riverside, Riverside, California, USA, 92951.

[2]Center for Earthquake Research and Information, University of Memphis, Memphis, Tennesse, USA

Corresponding Author: Baoning Wu (bwu015@ucr.edu). Address: 900 University Ave, Department of Earth and Planetary Sciences, University of California, Riverside, CA, USA, 92521

Christodoulos Kyriakopoulos is now at Center for Earthquake Research and Information, University of Memphis, Memphis, Tennesse, USA

Abstract

In this paper, we analyze the change in anthropogenic seismic noise level within a frequency range of 4-14 Hz through a survey of seismic stations in California, USA, New York City, USA, and Mexicali, Baja California, Mexico from early December, 2019 to late April, 2020. Our analysis shows that some stations recorded a drop in anthropogenic seismic noise during the COVID-19 pandemic, and the timing of the anthropogenic noise

decrease typically correlates with the timing of a strict curtailment of personal and economic activity issued by the local government. In other locations, the drop in the anthropogenic seismic noise appears not to follow the lockdown timing perfectly. During our analysis we observed that many stations did not record a drop during the early stage of COVID-19 pandemic. Of the 19 stations of the Southern California Seismic Network that were surveyed, we found that only five show a similar extent of drop in anthropogenic seismic noise comparable to the Christmas holiday break in 2019. This suggests that the human activity that caused seismic noise did not significantly reduce during the COVID-19 pandemic near most surveyed stations in Southern California. A further analysis implies that the primary seismic noise source in Southern California might be traffic, and the continuation of industrial traffic, such as cargo transportation, during the COVID-19 pandemic may be the reason why many stations did not record a noise drop. Our results show that the anthropogenic seismic noise recorded by seismic stations is capable of indicating human activity, and that this metric is particularly powerful in measuring how localized communities initially responded to the COVID-19 pandemic.

Introduction

The COVID-19 pandemic caused both tremendous economic hardship as well as reductions in human activity (e.g., Kraemer et al., 2020; Bonaccorsi et al., 2020). At the time of manuscript preparation (Nov. 14, 2020), the total confirmed number of COVID-19 cases has reached 11 million in the United States with 100 thousand more new cases reported each day. This devastating disease first struck the United States in late January, 2020 with its first arrival in the states of Washington and California. Soon, it developed into a nationwide pandemic in March, and New York State became the new “hotspot” of COVID-19. To prevent the overloading of hospitals, the state of California and New York took strong mitigation measures to enforce social distancing, hoping to slow the spread of virus and “flatten the curve” of daily confirmed cases (e.g., Matrajt et al., 2020; Thunström et al., 2020). At about the same time, the pandemic also spread in the neighbouring country of Mexico. Research has shown that the amplitude of human activity in a city can be correlated with the amplitude of seismic noise near populated areas (e.g., Lecocq et al., 2020; Gibney, 2020; Poli et al., 2020; Xiao et al., 2020). In the current research, we revisit the early stage of the COVID-19 pandemic in California, USA, New York City, USA, and Mexicali, Baja California, Mexico with seismic cultural noise recorded by seismic stations.

Human activity has a well demonstrated ability to generate seismic noise. Such noise can originate from traffic and machinery, and usually has frequency greater than 2–4 Hz (e.g., Stutzmann et al., 2000; McNamara and Buland, 2004; Havskov and Alguacil, 2015). Since anthropogenic, or cultural, seismic noise is rapidly attenuated (on the scale

of m to km from the source) due to its low amplitude and high frequency content, a seismometer is typically only sensitive to human activity within a range of a few kilometers (Havskov and Alguacil, 2015). Therefore, seismic data has the potential to provide us with unique information, which we can use to infer how a local community responds to the COVID-19 pandemic.

In this paper, we compute the seismic noise amplitude at 4-14 Hz at several seismic stations in California, USA, New York City, New York, USA, and Mexicali, Baja California, Mexico from early December, 2019 to late April, 2020, during which time cases of COVID-19 increased in the United States and Mexico, and strong social-distancing measures were taken by their respective governments. In this study we show that the seismic noise amplitude at 4-14 Hz reflects the human activity specific to the surrounding local community within a few kilometers' range. At some surveyed stations, a drop in anthropogenic seismic noise is observed concurrently with a social distancing measure in the area. This is consistent with the high frequency seismic noise quieting observed at the global scale (Lecocq et al., 2020). However, many stations we surveyed did not record a drop in seismic noise amplitude as had been expected, even though they were near population centers. Our results suggest that the seismic noise amplitude at 4-14 Hz is strongly affected by the human activity at a very local scale (within a few kilometers), and analyzing the patterns in these records may provide unique information on the human behaviors very close to these urban-region stations.

Methods

Measure seismic noise amplitude with displacement root mean square (RMS)

To measure the seismic noise amplitude within a given time window (from t=0 to t=T) at a certain frequency band (from f_1 to f_2), we compute the root mean square (RMS) amplitude u_{RMS} of the displacement seismogram $u(t)$ from t=0 to t=T at f_1-f_2 frequency band. A comprehensive description of our procedures can be found in the supplementary material (Text S1). Here we will only show a brief summary to illustrate the related concepts. The square of u_{RMS} can be defined as,

$$u_{RMS}^2 = \frac{1}{T}\int_0^T u^2(t)\mathrm{d}t$$

The root mean square amplitude u_{RMS} at a certain frequency band f_1 - f_2 is computed by integrating the power density spectrum $P(\omega)$ of displacement seismogram between t=0 and t=T, using Parseval's Theorem,

$$u_{RMS}^2 = \int_{f_1}^{f_2} P(\omega)\mathrm{d}\omega$$

To investigate how the seismic noise amplitude changes with time at a given station, we use a 30-minute sliding window (i.e., T=30 minutes) to scan through its continuous record. Considering that anthropogenic seismic noise is usually found in a frequency range greater than 2-4 Hz (Havskov and Alguacil, 2015), we compute the displacement root mean square amplitude u_{RMS} in a 4-14 Hz frequency band ($f_1 = 4$ Hz, $f_2 = 14$ Hz). The sliding window is offset by 15 minutes every time it advances. By scanning the continuous seismic data with the moving time window described above, we obtain a displacement RMS time-series with a sampling interval of 15 minutes. This time series is capable of showing cultural noise variation within a day.

However, the day-to-day variation of amplitude is not clear in the time series with a sampling rate of 15 minutes. In addition, short-duration (within a few seconds) tectonic events such as earthquakes can occur occasionally in the continuous dataset and make the direct analysis difficult. In order to compute the daily seismic noise amplitude, we take the median value of the 15-minutes-interval displacement RMS time-series of a certain day as the seismic noise amplitude of that day. We take the median of displacement RMS, rather than the average, to provide a representative value, since the median is less affected by outliers such as seismic events, allowing us to exclude earthquake effects in our analysis without explicitly removing them from our data. In the daily median displacement RMS time series, we have a single data point per day (i.e., sampling rate is one day) and we neglect the human activity variation within a day.

Determining the direction of maximum horizontal amplitude ϕ

To discriminate between noise sources, we determine the direction ϕ of the maximum horizontal displacement seismogram amplitude, measured clockwise from north. We use it as a potential indicator for noise source direction. We use the processing procedure developed in Tanimoto et al (2006). Here we demonstrate only the key concepts; the detailed procedures can be found in the supplementary materials (Text S2). We use a 30-minute sliding window to scan through the continuous record with an overlap of 15 minutes. For a given 30-minute time-series, we first compute the Discrete Fourier Transform of north and east component displacement seismograms $\boldsymbol{N}(\omega_i)$ and $\boldsymbol{E}(\omega_i)$. Then, we find the direction ϕ that maximizes the following quantity I,

$$I = \sum_{\omega_i=4\ Hz}^{14\ Hz} |\boldsymbol{N}(\omega_i)\cos\phi + \boldsymbol{E}(\omega_i)\sin\phi|^2$$

I, as a function of ϕ, repeats every 180˚; therefore, we define $\phi \in [0^\circ, 180^\circ)$. We denote ϕ_m as the direction that yields the maximum I_m. If the seismic noise at 4-14 Hz is primarily Rayleigh waves in horizontal component seismograms, ϕ_m or $\phi_m + 180^\circ$ would indicate the direction that noise comes from. However, unambiguously proving that the noise in our horizontal component seismograms at 4-14 Hz is due to Rayleigh waves is non-trivial and is beyond the scope of our paper. Therefore, we assume in this study that the seismic noise is predominantly Rayleigh waves and only use ϕ_m as a potential indicator for noise source direction.

Ambient noise cross-correlation

We also use ambient noise cross-correlation to indicate the noise source direction is. As supporting evidence, we calculate the Z component cross-correlation of one station pair, CI.RSS and AM.R2FCF. Rather than finding the travel-time information in the cross-correlation function, our goal is to find asymmetric pulses in the cross-correlation function, from which we can learn the dominant noise propagation direction between two stations. Our data preparation and cross-correlation procedures follow Benson et al. (2007) with some modifications. We use the raw vertical seismograms from January-01-2020 to March-15-2020 for both stations, cut to multiple time-series with length of 1 day, remove instrument response to displacement, remove mean, remove trend, and band-pass filter at 4-14 Hz. We then apply the “one-bit” normalization to the seismogram, which retains only the sign of the raw signal by replacing all positive amplitudes with 1 and all negative

amplitudes with -1. This procedure reduces the effect of the cross-correlations of earthquakes, instrumental irregularities, and nonstationary noise sources near stations. Finally, we compute the cross-correlation of each day and stack them. We do not perform the spectral whitening procedure in Benson et al. (2007).

Results

We divide the Results section into three parts. We first demonstrate an example of station BK.BRK to show the workflow of calculating seismic noise amplitude. This station has been investigated by Lecocq et al. (2020) and a lockdown noise reduction is observed. We then analyze the seismic noise amplitude at 4-14Hz at 23 stations in Southern California, United States to demonstrate the spatial variability of seismic noise drop during the COVID-19 lockdown. Lastly, we analyze two more stations outside California within the same period for comparative purposes: LD.CPNY at Central Park in New York City, United States and BC.UABX at downtown Mexicali, Baja California, Mexico.

Seismic noise drops due to government restrictions: an example from station BK.BRK in Berkeley, California

To demonstrate the workflow, we will show an example with station BK.BRK. BK.BRK is a seismic station on the campus of the University of California, Berkeley (Figure 2a and 2b), located within the city of Berkeley in the San Francisco Bay Area of California, one of the most densely populated areas in the United States. Lecocq et al. (2020) has observed a lockdown noise reduction at this station. In Figure 1, we show a

1-hour seismic record (06:00-07:00) from station BK.BRK. We consider 3 windows for this 1-hour record – from 06:00 to 06:30, 06:15 to 06:45, and 06:30 to 07:00. Within each time window, the displacement RMS amplitude u_{RMS} is computed between 4-14 Hz. The results are then used to represent the displacement RMS amplitude at the center of each time window, i.e., 06:15 for time window 1, 06:30 for time window 2, and 06:45 for time window 3.

We compute the displacement RMS of station BK.BRK from Dec 1, 2019 to Apr 26, 2020, and the results are shown in figure 2c. The thin black curves are the displacement RMS of the 30-minute-long sliding window, and the thick red curves show the median displacement RMS amplitude for the entire day. Before using the displacement RMS to indicate human activity, we need to first confirm that the ground vibration amplitude is primarily anthropogenic. We can confirm this claim by examining three patterns in the displacement RMS time series:

1. Daily pattern: as shown in figure 2c, the 15-minute-interval displacement RMS time series shows a strong diurnal periodic pattern. For the month of February, 2020, within each 24 hour cycle, the displacement RMS has a peak amplitude of about 2 nm during the daytime, and a minimum amplitude of about 1 nm during the nighttime.
2. Weekly pattern: the daily median of displacement RMS shows a strong weekly periodic pattern: it has a peak amplitude of about 1.5 nm during weekdays and a minimum amplitude of about 1.1 nm during weekends. These daily and weekly patterns reflect the prevailing mode of human activity: high in the daytime/weekdays and low in the nighttime/weekends.

3. Modulation of the weekly pattern in the holidays: during the Christmas and New Year's holiday in 2019, the ground vibration amplitude dropped about 30%, and the weekly pattern was modulated by the holiday schedule, suggesting a significant decrease in human activity during the public holidays.

Any of the displacement RMS patterns above alone might not be compelling enough to support an anthropogenic origin. However, when all three of the patterns co-exist, we consider it highly likely that the displacement RMS is dominated by anthropogenic noise. In this paper, we only use the displacement RMS time series for which all three of these patterns indicate the dominance of human activity in the seismic noise. Figure S1 shows the same data as Figure 2c except that the y-axis is extended to include the maximum displacement RMS of the 30-minute-long sliding window. The extreme values shown in Figure S1 are caused by earthquakes that infrequently occur. However, these occasional earthquakes do not affect the daily median displacement RMS, and thus will not saturate the low amplitude anthropogenic noise signal we study.

Once we confirm the dominance of anthropogenic signals in seismic noise, we move forward to investigate the human activity change around the time when social distancing restrictions were issued in March, 2020 at BK.BRK. As shown in the daily median displacement RMS time series in Figure 2c, the weekday daily median displacement RMS at station BK.BRK was about 1.5 nm in early December, 2019. It dropped to about 1 nm during the Christmas holiday and New Year's holiday. The weekday daily median displacement RMS gradually recovered back to its pre-holiday level in mid-January and stayed at that level until early March.

California was one of the first states in the United States to be affected by the COVID-19 pandemic. The first COVID-19 case was reported by the Center for Disease Control (CDC) on January 26, 2020 in Orange County (e.g., Linder, 2020; Wigglesworth et al., 2020). As the pandemic intensified in early March, strict restrictions on human activities were ordered by both local and state governments to stop the spread of the virus (e.g., California Office of the Governor, 2020; Casiano, 2020; Wick, 2020). On March 10, UC Berkeley suspended most in-person classes (Berkeley News, 2020), and the daily median displacement RMS at BK.BRK started to drop (Figure 2c). At midnight on March 17, a shelter-in-place order took effect in the Bay Area (Public Health Department, County of Santa Clara, 2020), and the daily median displacement RMS at 4-14 Hz underwent a further drop to about 1 nm on weekdays. This level is comparable to that of the 2019 Christmas/New Year holiday. The daily/weekly periodic pattern still persisted afterwards, suggesting that cultural noise is still the major contributor of the displacement RMS. Note that human activity is usually not observed in seismic noise beyond a few km from its source (e.g. Havskov and Alguacil, 2015), therefore this result, at the very best, can only directly constrain human activity in the immediate vicinity of the station BK.BRK. In Figures 2a and 2b, we use a blue circular shading to denote an area within 2 km of the station. This radius is a first-order empirical estimate of the range of anthropogenic noise sources.

As shown in the case of station BK.BRK, the daily median displacement RMS time series shows a clearer daily trend of human activity compared to the 15-minute-interval time series. In the remainder of this paper, we will only show the daily median

displacement RMS time series. The 15-minute-interval time series is not shown, although it was used to check if a diurnal periodic pattern exists.

Spatial variability of seismic noise drops during a shelter-in-place order in Southern California

Southern California is one of the most densely populated regions in the United States. It also has one of the densest seismic networks in the world due to the proximity of the San Andreas fault and other dangerous structures in the Pacific-North America plate boundary zone. The Southern California Seismic Network (Network code: CI) is the largest seismic network in Southern California, operated by the California Institute of Technology (Caltech) and the United States Geological Survey (USGS) in Pasadena (California Institute Of Technology And United States Geological Survey Pasadena, 1926). Many stations within this network are close to or within significant population centers, and they provide a valuable dataset to study the human activity drop patterns in Southern California during the COVID-19 pandemic.

We investigate the displacement RMS amplitude at 23 seismic stations in Southern California to obtain an accurate picture of human activity change in the region. The locations of these analyzed stations are shown in Figure 3. We use the three criteria established in the previous analysis of BK.BRK to examine whether the seismic noise at a given station is dominated by anthropogenic sources. Out of the 23 stations, 19 of them show a diurnal/weekly cycle and a reduction of signal over Christmas, which is indicative of changes in anthropogenic seismic noise. As will be discussed later, the other 4 stations do not reflect obvious anthropogenic characteristics (Figure S4).

To directly compare the 19 time-series that reflect human activity, we scale them using the following method: For a given time-series, we define the “0” level as the mean of the daily median displacement RMS during Christmas/New Year break (12/21/2019 – 01/06/2020). We define the “1” level as the mean of the daily median displacement RMS during a non-holiday period (01/20/2020 – 02/29/2020). After that, the time-series is normalized using the pre-defined “0” and “1” level. If a time series has amplitude closer to 0 after the shelter-in-place order, it means that the daily median displacement RMS amplitude dropped close to the “Christmas” level; Conversely, if a time series has amplitude closer to 1 after the stay-at-home order, it means that the daily median displacement RMS amplitude remained at the normal non-holiday level.

In Figure 4a, we plot all the 19 traces together. The green horizontal dashed line denotes the Christmas/New Year holidays level, and the orange horizontal dashed line denotes the normal non-holiday level. In California, a statewide shelter-in-place order was declared on March 19, 2020 (e.g., Casiano, 2020; Wick, 2020; Arango and Cowan, 2020). As shown in Figure 4a, the patterns of all traces are very similar before the shelter-in-place order on March 19. However, the seismic noise amplitude at 4-14Hz at different stations starts to diverge after March 19. 14 of the 19 stations remained at the normal non-holiday level, while the remaining 5 stations dropped close to the Christmas level. In Figure 4b, we plot the 5 stations that show an amplitude drop in red and the other 14 stations that do not show drop in black. The 5 stations have very similar trends to the other 14 stations before the shelter-in-place order in California.

The result above demonstrates a clear spatial variability in anthropogenic seismic noise drop in Southern California after the California shelter-in-place order. The

anthropogenic seismic noise level at many locations in Southern California surveyed in this study (14 out of 19) did not decrease after the “stay-at-home” order in contrast to the well-resolved reduction in noise level observed during the Christmas/New Year’s holiday. Since anthropogenic seismic noise mainly originates from traffic and machinery (e.g., Stutzmann et al., 2000; McNamara and Buland, 2004; Havskov and Alguacil, 2015), it might imply that the traffic or industrial activities in Southern California did not significantly change after the “stay-at-home” order was enacted. We will further discuss these results in the Discussion section.

Seismic noise changes in Central Park, New York City and downtown Mexicali, Mexico

The results above suggest that the anthropogenic seismic noise recorded by a seismometer can be used as an indicator of human activity for the nearby community. It is worth noting that the displacement RMS amplitude at many stations in Southern California did not show a drop concurrent with the timing of California’s stay-at-home order. This result highlights a unique benefit of using seismic noise amplitude to indicate human activity in that it reflects the human activity, and societal response to government measures, specific to the surrounding local community, instead of the whole city or state. In this section, we extend our investigation to two other stations outside California for comparative purposes: station LD.CPNY in Central Park in New York City (another population center in United states) and station BC.UABX on the campus of Autonomous University of Baja California (UABC) near downtown Mexicali, Baja California, Mexico (a Mexico city bordering Southern California). The locations of these two stations are shown in Figure 5a and 5b.

We compute the displacement RMS of station LD.CPNY and BC.UABX For reference, we compare them with the displacement RMS of station BK.BRK in Berkeley, California, which is discussed above. Figure 5c plots the daily median displacement RMS from Dec-01 to Apr-26 of these three stations. In the panel for each station, blue curves show the trend of the pandemic-affected year (Dec-2019 to Apr-2020) and gray curves show the trend of the previous year (Dec-2018 to Apr-2019) as a comparison. Vertical lines of different colors (numbered in a chronological order) denote the dates when potential human-activity-related measurements were issued, such as a “school closure” order or a “shelter-in-place” order.

As shown in Figure 5c, all three stations show a weekdays-weekend variation pattern in displacement RMS records. At station BC.UABX, a decrease in amplitude is concurrent with the Christmas (December 25) and New Year holiday (January 1) for both years. At LP-CPNY a decrease in amplitude during this same period is not observed, although the weekday/weekend periodicity does appear to be modulated, suggesting rapidly fluctuating changes in human activity. These results indicate that the seismic noise at these three stations is subject to nearby human activity and therefore are capable of reflecting human activity change. A more speculative reading of our results suggests that individual locations may respond to specific events differently, resulting in differences in the seismic noise record. As an example, we see that amplitude of seismic noise near Central Park (LD.CPNY) does not drop off near the Christmas holidays, in contrast to stations BC.UABX and BK.BRK. This might be due to the fact that human activity near the park did not decrease during holidays.

We then further investigate the displacement RMS amplitude before and after the COVID-19 pandemic. Before March 2020, the displacement RMS amplitudes at these three stations are very similar to the same period in the previous year. As the COVID-19 pandemic intensified in March 2020, displacement RMS began to drop to a level lower than in the previous year (the year 2019). Station BK.BRK on the UC Berkeley campus records a drop in displacement RMS amplitude starting from March 10 when UC Berkeley was closed, and continued to drop when the shelter-in-place order was issued in the Bay Area on March 17. At Central Park in New York City, station LD.CPNY records a slight drop of displacement RMS amplitude a few days before Governor Andrew Cuomo signed the 'New York State on PAUSE' executive order on March 20, closing 100% of non-essential businesses statewide (New York Office of the Governor, 2020). Displacement RMS decreased further when the order took effect on March 22. One week later, on approximately March 27, the displacement RMS amplitude of LD.CPNY dropped to its lowest level.

In the border town of Mexicali, station BC.UABX records a drop in displacement RMS amplitude on March 17. This drop occurred almost concurrently with the state-wide shelter-in-place order in California issued on March 19. On March 30 a shelter-in-place order was also issued in Baja California (the Mexican state where Mexicali is located) (e.g., Lewis, 2020; Fry, 2020), almost two weeks after the recorded displacement RMS amplitude dropped in Mexicali. This result shows that the change in the anthropogenic noise in downtown Mexicali is correlated with the shelter-in–place order in California, rather than the shelter-in-place order in Baja California. It suggests that human activity in Mexicali is probably strongly influenced by the bordering US state of California.

In summary, we find that although the two stations LD.CPNY and BC.UABX recorded a drop in seismic noise in March 2020, the drops did not perfectly coincide with the regional shelter-in-place order. The differences between the state orders and the displacement RMS time-series suggest that the independent measures of human activity are sensitive to different but complementary aspects of the pandemic response. The anthropogenic seismic noise should reflect the human activity level in the local area (within several kilometers). We will further discuss this point in the Discussion section.

Discussion

Spatial variability of seismic noise trends in Southern California

An interesting observation in our study is that the anthropogenic seismic noise trends in Southern California are spatially diverse after the “shelter-in-place” order was implemented. Anthropogenic noise dominates 19 out of the 23 stations we surveyed. As shown in Figure 4, all these 19 stations show very similar trends in displacement RMS time-series before the “shelter-in-place” order; after that, 5 stations recorded a drop in displacement RMS amplitude while the other 14 did not. Figure 6a shows the comparison between the mean displacement RMS time-series of the 5 “drop” stations (red solid curve) and the mean displacement RMS time-series of the 14 “no drop” stations (black solid curve). We can see that the diverse modes in trends start from mid-March (around March 15). After that, the displacement RMS amplitude of the 5 “drop” stations decreases to near the Christmas/New Year break level; while the displacement RMS amplitude of the 14 “no drop” stations, still remains close to the non-holiday level. However a slight decrease is still visible within those 14 stations.

To further investigate this observation, we define the shelter-in-place anthropogenic noise level as the mean value of displacement RMS time-series between 03/20/2020 – 04/26/2020. In Figure 6b, we plot the scaled shelter-in-place noise level against the absolute non-holiday noise level for all 19 stations that are dominated by anthropogenic noise. All the 5 stations that we visually identify as having a noise drop after the COVID-19 shelter-in-place order have a scaled shelter-in-place noise level lower than 0.6, while for the other 14 stations the shelter-in-place noise level is higher than 0.6. It is worth noting that stations that recorded a noise drop during shelter-in-place tend to have a higher absolute noise level during the non-holiday period compared to 7 stations that did not record a noise drop. However, there are also 7 stations that have a high absolute noise level during the non-holiday period that did not record a noise drop as well. This result implies that having a high absolute noise level is necessary but not a sufficient condition for a station to record a noise drop in the shelter-in-place period. This point is further illustrated when we compare the seismic noise probability density function (PDF) among these 23 stations we survey in Southern California (method in supplementary martial, Text S3). Figure 6c shows the average power of the PDFs of these stations. All the 5 “drop” stations have a relatively high noise level at 4-14 Hz, although there are also 7 “no drop” stations have a similar high noise level as well.

Stations that are insensitive to anthropogenic noise sources

In southern California, we found 4 stations that did not show anthropogenic noise characteristics (CI.CJM, CI.DEV, CI.IPT, CI.PER). Their displacement RMS time-series are shown in Figure S4. Although all these 4 stations show some extent of anthropogenic

noise characteristics from time to time (diurnal/weekly periodic pattern), their patterns are not stable so we do not include them into our analysis.

A comprehensive discussion of why these stations are insensitive to anthropogenic noise sources is beyond the scope of this paper. Instead, we pose some hypotheses only based on the data we obtain in this study. As for station CI.CJM, CI.DEV, and CI.IPT, they are located relatively far from a population center or a dense road network (Figure 3), so the anthropogenic noise they receive is relatively low (Figure 6c). In addition, station CI.CJM, CI.DEV, and CI.IPT are relatively close to the San Andreas Fault (within a few kilometers), and the earthquakes nearby may greatly contribute to seismic noise at 4-14 Hz and swamp the anthropogenic noise (Figure S4a to S4c). As for station CI.PER, it is neither far away from a population center nor very close to an active fault. However, the baseline of its seismic noise level at 4-14 Hz seems to have a very long period oscillation (Figure S4d). On top of this long period oscillation, diurnal and weekly periodic patterns can still be occasionally seen. We are not clear why this long period oscillation exists.

Nevertheless, we note that our hypotheses here are very preliminary and speculative. A thorough study on these null stations is needed in the future before their behavior can be fully explained.

Traffic as the origin of anthropogenic noise source in Southern California

Considering that anthropogenic seismic noise at 4-14 Hz are usually not detected beyond a few kilometers, the 19 stations that show anthropogenic noise characteristics are likely to have noise sources that are different from each other. Since the displacement RMS of those 19 stations have an almost identical pattern before the shelter-in-place

order (Figure 4), it suggests that the human activities that generate 4-14 Hz anthropogenic noise in Southern California might share very similar characteristics at different locations and might be stable through time. Therefore, the variation we see in a station might not come from a noise source that is unique to the locality, such as a generator or air condition very close to the station, or a noise source that is transient, such as a nearby construction site in operation for only a short period of time.

A plausible explanation we favor for the noise source is traffic. In Southern California, traffic is relatively homogeneous throughout the region. If traffic were the major anthropogenic noise source, it would cause similar noise level trends at different stations far apart. In addition, traffic conditions in Southern California are stable through time and therefore the weekly pattern in its seismic noise should be stable through time as well. These characteristics are consistent with the displacement RMS trends we observe in Southern California, making traffic an attractive candidate explanation.

A comprehensive investigation to confirm the noise source could be non-trivial. Since noise above 4 Hz usually cannot be recorded beyond a few kilometers from the source, the local human activity condition around a station must be well characterized to make a detailed analysis. A systematic detailed analysis of the noise sources at all the stations we survey will be a subject for a future study. In this part of discussion, we will pick three of our surveyed stations to analyze as an example: CI.MSJ, CI.RVR and CI.RSS. CI.RVR and CI.RSS are capable of reflecting human activity, yet CI.MSJ recorded a drop in human activity after the shelter-in-place order while CI.RSS did not. Since these three stations are within the Riverside area where all the authors of this paper

are based, we feel relatively comfortable to speak about the human activity in the region both before and after the pandemic.

To investigate the noise source at the different stations, we determine the direction of maximum horizontal amplitude ϕ_m (with respect to north) of the three stations between 02/10/2020 – 02/24/2020, a two-week non-holiday period before the shelter-in-place order. CI.RVR is another station we surveyed near the Riverside region that did not record a drop in anthropogenic noise. Figure 7a and 7b show the direction ϕ_m on map. The orientation of a line centered at a station denotes the direction ϕ_m and the length of line represents the normalized amplitude I_m. Gray thin lines show the ϕ_m of 1469 segments within this period and the red thick line shows the mode of direction ϕ_m. Figure 7c to 7e show the histogram of direction ϕ_m of these three stations, with the red line denoting the mode of direction ϕ_m.

If we assume that the horizontal polarities in our results are mainly caused by Rayleigh wave, the direction ϕ_m or $\phi_m + 180°$ could indicate the direction where noise is coming from. If this assumption were true, our results would strongly suggest that the anthropogenic noise is coming from traffic in the three stations we investigate. For station CI.MSJ, the mode of direction ϕ_m is 16˚. It is perpendicular to the California State Route 79 and the direction $\phi_m + 180° = 196°$ is approximately pointing to the junction where the California State Route 79 intersects two other major local roads. The histogram of CI.MSJ implies that ϕ_m occasionally changes to about 120˚, and the direction $\phi_m + 180°$ is 300˚. This direction is perpendicular to a very close major local road that runs north-south. At station CI.RVR and CI.RSS, the modes of direction are 20˚ and 86˚. These two directions

454 are perpendicular to the nearby California State Route 60, where the traffic is the busiest
455 and most crowded near the Riverside area. Noticeably, direction ϕ_m rotates as the
456 California State Route 60 makes a slight turn from east to west, and the rotation angle is
457 similar to the road turning angle. This pattern again supports that the anthropogenic noise
458 at 4-14 Hz at these two stations originated from traffic.

459 The above single-station analysis indicates that traffic is the major source of 4-14
460 Hz seismic noise at these stations, yet it relies on the assumption that the noise is
461 Rayleigh wave. Ambient noise cross-correlation is a helpful tool to investigate the noise
462 source direction; yet the frequency band we study is so high that even for a close station
463 pair of CI.RSS and CI.RVR that are 5 km apart, their ambient noise did not correlate
464 (figure S2). Fortunately, there is a Raspberry Shake station AM.R2FCF that is only 1.6
465 km away from the station CI.RSS (Figure 7b). Although it only has a vertical component
466 and the accuracy is not as good as a permanent station, this station makes an ambient
467 noise cross-correlation investigation at 4-14 Hz possible. Figure 7f shows the cross-
468 correlation function between CI.RSS.BHZ and AM.R2FCF.EHZ. The gray lines denote
469 the day-correlation function of each 14 day and the purple line denotes the stack
470 correlation function. There are wave packets of large amplitude on the negative time axis
471 at around -2.8s, while there are not such packets on the positive time axis. This result
472 suggests that the dominant correlated noise at these two stations mainly propagates from
473 CI.RSS to AM.R2FCF. This is consistent with our hypothesis that the noise at CI.RSS
474 comes from the California State Route 60. A lag time of 2.8 s of these wave packets and
475 a station separation of 1.6 km imply an average group velocity of 0.57 km/s, suggesting
476 that these wave packets might be the fundamental Rayleigh waves.

The last piece of evidence that supports the traffic hypothesis comes from the comparison with precipitation data. In Figure 8, we compare the average displacement RMS with the average daily precipitation in Southern California during the same period (the method to compute the average daily precipitation of Southern California can be found in the supplementary material Text S5). All of the seismic stations sensitive to human activity, whether their displacement RMS dropped during the COVID-19 lockdown or not, show a drop during the second week in April (April 05 – April 11). This drop correlates with a period of heavy precipitation in Southern California (Figure 8). This correlation could potentially be explained by traffic drop caused by an unfavorable weather condition. In the same period, the four stations that do not appear to be sensitive to human activity variation show no drop in displacement RMS amplitude (Figure S4), meaning that the drop of displacement RMS amplitude in Figure 8 during the week of April 05 through April 11 probably is not due to a change in subsurface seismic structure induced by the increase of rainfall.

In summary, traffic activity appears to be able to explain all the observations we have so far; therefore, we consider the traffic activity to be the major noise source at 4-14 Hz for the 19 stations that show anthropogenic noise characteristics. This hypothesis can be further tested in a future study.

Why does the anthropogenic noise source not drop in many Southern California stations?

Our results suggest that the behaviors of anthropogenic seismic noise after the shelter-in-place order are very diverse. If we assume that the level of anthropogenic

seismic noise is at least somewhat proportional to the level of the human activity that causes it, our results above would imply that the seismic-noise-causing human activities responded differently to the shelter-in-place order at different locations. Near the vicinity of some stations, these human activities drop during the shelter-in-place as they did in the Christmas/New year break; while for others these human activities did not drop. What is the reason behind this spatial variability?

It is non-trivial to fully address this question across the whole dataset. Here, we propose a hypothesis based on the comparison between CI.MSJ and CI.RSS and on the authors' experience in the Riverside area. As shown in Figure 9a, CI.MSJ is located on the Mt. San Jacinto College (MSJC) campus and the CI.RSS station is located on the University of California, Riverside (UC Riverside) campus. Figure 9b plots the daily median displacement RMS time-series of these two stations. The top panel is CI.MSJ and the bottom panel is CI.RSS. Blue curves show the trends of the pandemic affected year (Dec 2019 to Apr 2020) and gray lines show the trends of the previous year in the same period (Dec 2018 to Apr 2019). In both the time-series of CI.MSJ and CI.RSS, displacement RMS dropped to a low level during the 2019 Christmas holiday and gradually climbed back to a high level in January 2020. As the COVID-19 situation intensified in early March 2020, Mt. San Jacinto College closed its campus on Friday, March 13 (Schultz, 2020). On March 16, UC Riverside also closed its campus (Smith, 2020). Purple dashed lines denote the timing of when the two schools closed their campuses. Both of the campuses closed after the shelter-in-place order. However, the displacement RMS time-series only shows a significant drop in amplitude on the CI.MSJ record, not on the CI.RSS record.

As we discuss earlier, traffic activities would most likely be the noise sources at CI.MSJ and CI.RSS. If that is the case, why does the traffic activity drop near CI.MSJ while not in CI.RSS, even though they are only 40 km apart? We propose that it is because of the difference in traffic type. Immediately adjacent UC Riverside are California State Routes 60 and 91, and Interstate Highway 215, all of which are designated as part of the Primary Freight Network System of the United States (link of the map provided in Data and Resources section), which the Federal Highway Administration defines as “the most critical highway portions of the U.S. freight transportation system determined by measurable and objective national data”. The traffic related to such essential activities may not reduce after the shelter-in-place order. The nearest highway to Mt. San Jacinto College is located over 10 miles away, and therefore the noise at the station may be mainly related to local traffic, which may have been more strongly affected by the shelter-in-place order. This hypothesis can be tested more comprehensively in a future study.

Comparing displacement RMS time-series with Apple mobility "driving index"

There are some independent datasets on human activity that are provided by smartphone-based mapping services. These smartphone-based mobility index reflect the human activity in the larger metropolitan area, while the displacement RMS should reflect the human activity level in the local area (within several kilometers). Therefore, it might be beneficial for us to compare these two similar but different types of dataset. Here we compare our displacement RMS time-series with the Apple mobility "driving index". The Apple mobility "driving index" is one of the mobility trends released by the Apple Inc, which are calculated based on the requests for directions in Apple Maps (details in the Data and Resources section). The data show a relative volume of direction requests per

country/region, sub-region or city compared to a baseline volume on January 13th, 2020. Details about what city/sub-region we select can be found in the supplementary materials (Text S4).

In Figure 6a, we compare our displacement RMS trends in Southern California with the Apple mobility "driving index" of Los Angeles City (blue dashed curve). The Apple mobility "driving index" is similar to the displacement RMS. It has a weekly periodic pattern that its amplitude is high on weekdays while low on weekends. Noticeably, the Apple mobility "driving index" always gradually increases during the weekdays and peaks on Fridays, which is different from the flat weekday-trend observed in displacement RMS. A robust determination of this difference is out of the scope of this paper. After the shelter-in-place order was implemented, the Apple mobility "driving index" dropped about 50%, implying that the average driving activity in the region was reduced in compliance with the order. However, as we discussed earlier, the displacement RMS only drops in some stations while not in many others.

To further investigate the difference between seismic and smartphone-based data, we compare the displacement RMS with the Apple mobility "driving index" for the three stations we investigate in the last Result subsection: BK.BRK, LD.CPNY and BC.UABX (Figure 10). As shown in the figure, the displacement RMS drops recorded by seismometers are consistent with the decrease in Apple mobility "driving index" in general. The differences in details may reflect the particular conditions in the local area near the seismometer. For example, the Apple mobility "driving index" in Baja California started to drop several days earlier than the displacement RMS in downtown Mexicali. Likewise, the Apple mobility "driving index" in New York City shows a minimum in activity on around

March 20, while the displacement RMS at LD.CPNY near Central Park reached its lowest level one week later on around March 27.

The differences between the Apple Mobility Trend data and the displacement RMS time-series suggest that the independent measures of human activity are sensitive to different but complementary aspects of the pandemic response. The displacement RMS should reflect the human activity level in the local area (within several kilometers), while the Apple Mobility Trend should reflect human activity in the larger metropolitan area. By considering both the similarities and differences it may help us to better characterize human behavior to the pandemic.

Conclusions

In this article, we use seismic data to extract information on human activity changes during the early stage of the global COVID-19 pandemic in California, USA, New York City, USA, and Mexicali, Baja California, Mexico. We show that the displacement RMS at 4-14 Hz has the ability to monitor human activity at a very local (several kilometers range) scale. While these data are to first-order consistent with mitigation measures of the greater metropolitan area, the ground motion data reveal unique information about the local area. In Southern California, we observe that while some stations record a drop in human activity comparable to the Christmas holiday period, most stations do not. Considering the similarity in displacement RMS time series between different stations, and some evidence that indicate the noise back-azimuth, we argue that traffic activities are very likely the noise source at 4-14 Hz for the 19 stations that show anthropogenic noise characteristics. Based on this argument, we propose that it is the difference in traffic

590 type that determines whether the seismic noise drops near a station or not. For stations
591 like CI.RSS, their nearby traffic activities include significant freight traffic. This traffic is
592 likely related to essential activities and may not reduce after the shelter-in-place order.
593 Conversely for stations like CI.MSJ, nearby traffic activities are likely dominated by
594 commuter traffic. Such traffic may be strongly affected by the shelter-in-place order and
595 the displacement RMS would drop.

596 We investigate two other stations outside California, USA: station LD.CPNY in
597 Central Park, New York City, USA and station BC.UABX near downtown Mexicali, Baja
598 California, Mexico. The drop in displacement RMS of LD.CPNY near the Central Park
599 area in New York City is delayed by approximately one week from the decrease in human
600 activity in New York City determined by the Apple mobility "driving index". Station
601 BC.UABX records a drop in human activity during the COVID-19 pandemic. However, the
602 timing of its drop is better correlated with the date of shelter-in-place order in its
603 neighboring US state of California, rather than the date of implementation of shelter-in-
604 place order in Mexico. These results suggest that the displacement RMS is sensitive to
605 very localized human activity change and is thus capable of helping us better characterize
606 the human behavior in response to COVID-19 pandemic.

607 Although a seismometer is best known for its ability to record earthquake shaking,
608 it is also capable of recording ground movements caused by human activity, as we
609 explore in this article. In particular, we have shown that the seismic noise at 4-14 Hz is
610 particularly sensitive to the human activity changes at a very local (several kilometers
611 range) scale. The reduction in human activity during the pandemic offers us a chance to
612 explore the nature of anthropogenic seismic noise in the seismic record, such as its

physical origins and its attenuation with distance. In addition, the advancements of open-access seismic data make it possible for a daily monitoring of human activity via seismic noise in near real-time, as opposed to a smartphone-based mobility index that could have a data lag of a couple of weeks. If interpreted properly, the seismic noise data can provide useful information on human activity that responds to the pandemic at a very local scale.

Data and Resources

All seismic data we used are open-access at different data centers and can be accessed through the Incorporated Research Institutions for Seismology (IRIS) website (www.iris.edu, last accessed June 2020). The data of Southern California Seismic Network (CI) is downloaded from the Southern California Earthquake Data Center (SCEDC). The data of Berkeley Digital Seismograph Network (BK) is downloaded from the Northern California Earthquake Data Center (NCEDC). The data of Lamont-Doherty Cooperative Seismographic Network (LD), CICESE's Seismic Network (BC) and Mexican National Seismic Network (MX) are downloaded from the IRIS Data Management Center (IRISDMC). The Apple Mobility Trends data are downloaded from https://www.apple.com/covid19/mobility, last accessed May 02, 2020. The precipitation data in Southern California is downloaded from the National Weather Service (NWS) Office website (https://w2.weather.gov/climate/xmacis.php?wfo=lox for Los Angeles/Oxnard Office data, last accessed June 2020; https://w2.weather.gov/climate/xmacis.php?wfo=sgx for San Diego Office data, last accessed June 2020). All maps in the paper are made with Google Maps (https://www.google.com/maps, last accessed July 2020). The map of the Primary Freight

Network System of the United States can be found on https://ops.fhwa.dot.gov/freight/infrastructure/ismt/state_maps/states/california.htm

This paper contain a Supplementary Materials document (a word document). It includes 1. (Text S1) details of the method to compute displacement RMS. 2. (Text S2) details of the method to determine the direction of maximum horizontal amplitude. 3. (Text S3) the method to calculate the seismic noise probability density function (PDF). 4. (Text S4) details about how we select a city/sub-region in the Apple Mobility Trends Reports. 5. (Text S5) how we compute the average daily precipitation of Southern California. 6. (Text S6) a brief review of social-distancing measures in our study region that are potentially related to the timing of seismic noise drop. 7. (Figure S1) the same figure as Figure 2c except that the y-axis is extended to include the maximum displacement RMS of the 30-minute-long sliding window. 8. (Figure S2) Cross-correlation function between CI.RSS and CI.RVR. 9. (Figure S3) instrument response functions. 10. (Figure S4) the displacement RMS time-series of the 4 stations that are not capable of reflecting human activity variation.

Acknowledgments

We are grateful to Daniel McNamara and Stephen Hicks for constructive reviews that greatly improved the manuscript. This research was initiated and developed in the seismology journal club at Earth and Planetary Sciences Department at University of California, Riverside. We want to thank all the participants (and their families and friends!) for discussing the results and providing input with their life experience in the study area.

We thank Dr. Thomas Lecocq for sharing the SeismoRMS code package and making a very easy-to-understand Jupyter Notebook tutorial for everyone.

References

Apple Mobility Trends Reports, https://www.apple.com/covid19/mobility, Accessed May 02, 2020.

Arango, T., and J. Cowan (2020) Gov. Gavin Newsom of California Orders Californians to Stay at Home [online], *The New York Times*, March 19, 2020 Available at: https://www.nytimes.com/2020/03/19/us/California-stay-at-home-order-virus.html. Accessed July 20, 2020.

Bensen, G.D., M.H. Ritzwoller, M.P. Barmin, A.L. Levshin, F. Lin, M.P. Moschetti, N.M. Shapiro, and Y. Yang (2007). Processing seismic ambient noise data to obtain reliable broad-band surface wave dispersion measurements. *Geophysical journal international*, 169(3), pp.1239-1260.

Berkeley News (2020) As coronavirus spreads, UC Berkeley suspends in-person instruction [online], *University of California, Berkeley website*, March 9, 2020 Available at: https://news.berkeley.edu/2020/03/09/as-coronavirus-spreads-uc-berkeley-suspends-in-person-instruction/. Accessed July 21, 2020.

Bonaccorsi, G., F. Pierri, M. Cinelli, A. Flori, A. Galeazzi, F. Porcelli, A.L. Schmidt, C.M. Valensise, A. Scala, W. Quattrociocchi, and F. Pammolli (2020). Economic and social consequences of human mobility restrictions under COVID-19. *Proceedings of the National Academy of Sciences*, 117(27), pp.15530-15535.

California Institute Of Technology And United States Geological Survey Pasadena (1926). Southern California Seismic Network, *International Federation of Digital Seismograph Networks*, doi: 10.7914/SN/CI.

California Office of the Governor (2020) Governor Newsom Declares State of Emergency to Help State Prepare for Broader Spread of COVID-19 (Press release) [online], March 4, 2020. Available at: https://www.gov.ca.gov/2020/03/04/governor-newsom-declares-state-of-emergency-to-help-state-prepare-for-broader-spread-of-covid-19/. Accessed July 20, 2020.

Casiano, L. (2020) California Gov. Gavin Newsom announces statewide coronavirus 'stay at home' order [online], *Fox News*, March 19, 2020 Available at: https://www.foxnews.com/us/california-gov-gavin-newsom-announces-statewide-stay-at-home-order.amp?cmpid=prn_newsstand. Accessed July 20, 2020.

Fry, W. (2020) Baja California to use police and military forces to keep people inside [online], *The San Diego Union-Tribune*, March 30, 2020 Available at: https://www.sandiegouniontribune.com/news/border-baja-california/story/2020-03-30/baja-california-to-deploy-military-forces-to-keep-people-inside. Accessed July 21, 2020.

Gibney, E. (2020) Coronavirus lockdowns have changed the way Earth moves, *Nature*, 580(7802), p.176.

Havskov, J. and G. Alguacil (2015) *Instrumentation in Earthquake Seismology*, Chapter 3, Springer.

Kraemer, M.U., C.H. Yang, B. Gutierrez, C.H. Wu, B. Klein, D.M. Pigott, L. Du Plessis,, N.R. Faria, R. Li, W.P. Hanage, and J.S. Brownstein (2020) The effect of human mobility and control measures on the COVID-19 epidemic in China. *Science*, 368(6490), pp.493-497.

Lecocq, T. et al. (2020) Global quieting of high-frequency seismic noise due to COVID-19 pandemic lockdown measures, *Science* (80-.)., doi: 10.1126/science.abd2438.

Lewis, B. (2020) Baja California battling coronavirus, residents urged to stay home [online], *CBS 8*, April 1, 2020 Available at: https://www.cbs8.com/article/news/health/coronavirus/baja-california-battling-coronavirus-residents-urged-to-stay-home/509-26f77b1e-ae07-4aee-afc8-392ae74a3d10. Accessed July 21, 2020.

Linder, M. (2020) California's First Case of Coronavirus Confirmed in Orange County [online], *NBC Bay Area*, January 26, 2020 Available at: https://www.nbcbayarea.com/news/california/first-case-of-coronavirus-confirmed-in-californias-orange-county/2221025/. Accessed July 21, 2020.

Matrajt, L., and T. Leung (2020) Evaluating the Effectiveness of Social Distancing Interventions to Delay or Flatten the Epidemic Curve of Coronavirus Disease, *Emerging infectious diseases*, 26(8).

McNamara, D.E., and R.P. Buland (2004) Ambient noise levels in the continental United States, *Bulletin of the seismological society of America*, 94(4), pp.1517-1527.

New York Office of the Governor (2020) Governor Cuomo Signs the 'New York State on PAUSE' Executive Order (Press release) [online], March 20, 2020 Available at: https://www.governor.ny.gov/news/governor-cuomo-signs-new-york-state-pause-executive-order. Accessed July 20, 2020.

Peterson, J.R. (1993) Observations and modeling of seismic background noise (No. 93-322). *US Geological Survey*.

Poli, P., J. Boaga, I. Molinari, V. Cascone, and L. Boschi, 2020, The 2020 coronavirus lockdown and seismic monitoring of anthropic activities in Northern Italy, *Sci. Rep.*, 10, no. 1, 9404, doi: 10.1038/s41598-020-66368-0.

Public Health Department, County of Santa Clara (2020) Seven Bay Area Jurisdictions Order Residents to Stay Home (Press release) [online], March 16, 2020. Available at: https://www.sccgov.org/sites/phd/news/Pages/press-release-03-16-20.aspx. Accessed July 20, 2020.

Schultz, R. (2020) MSJC Closing All Locations Until 4/6 (School Announcement) [online], *Mt. San Jacinto College website*, March 13, 2020 Available at: https://www.msjc.edu/coronavirus/message-to-students-2020-03-13.html. Accessed July 21, 2020.

Smith, T. (2020) UCR Campus "Closed" (School Announcement) [online], *University of California, Riverside website*, March 14, 2020 Available at: https://insideucr.ucr.edu/announcements/2020/03/14/ucr-campus-closed. Accessed July 21, 2020.

739 Stutzmann, E., G. Roult, and L. Astiz (2000) GEOSCOPE station noise levels, *Bulletin*
740 *of the Seismological Society of America,* 90(3), pp.690-701.

741 Tanimoto, T., S. Ishimaru, and C. Alvizuri (2006) Seasonality in particle motion of
742 microseisms. *Geophysical Journal International*, 166(1), pp.253-266.

743 Thunström, L., S.C. Newbold, D. Finnoff, M. Ashworth, and J.F. Shogren (2020) The
744 benefits and costs of using social distancing to flatten the curve for COVID-19, *Journal*
745 *of Benefit-Cost Analysis*, pp.1-27.

746 Wick, J. (2020) Newsletter: Newsom to 40 million Californians: Stay home [online], *Los*
747 *Angeles Times*, March 20, 2020 Available at:
748 https://www.latimes.com/california/newsletter/2020-03-20/california-stay-home-newsom-
749 coronavirus-newsletter-essential-california. Accessed July 20, 2020.

750 Wigglesworth, A., R. Lin II, and S. Kohli (2020) California's first two cases of
751 coronavirus are confirmed in L.A. and Orange counties [online], *Los Angeles Times*,
752 January 26, 2020 Available at: https://www.latimes.com/california/story/2020-01-25/los-
753 angeles-area-prepared-for-coronavirus. Accessed July 21, 2020.

754 Xiao, H., Z. Eilon, C. Ji, and T. Tanimoto (2020) COVID-19 Societal Response Captured
755 by Seismic Noise in China and Italy. *Seismological Research Letters*; 91 (5): 2757–
756 2768.

Full mailing address for each author

Baoning Wu[1], Roby Douilly[1], Heather A. Ford[1], Gareth Funning[1], Hsin-Yu Lee[1], Shankho Niyogi[1], Manuel Mendoza[1], Christodoulos Kyriakopoulos[2], and David Oglesby[1]

[1]900 University Ave, Department of Earth and Planetary Sciences, University of California, Riverside, CA, USA, 92521

[2]3890 Central Ave, Center for Earthquake Research and Information (CERI), University of Memphis, TN, USA, 38152

Figure captions

Figure 1. An example of a seismic record demonstrating how the sliding time-windows are used to compute displacement root mean square (RMS) time series. The seismogram in red is 1 hour of a vertical component seismogram (BHZ) at station BK.BRK filtered at 4-14 Hz (from 2020-05-20, 6am to 7am, local time). The blue, cyan, and brown horizontal lines below the plot denote the three, 30 minutes long overlapping sliding time windows within this one hour.

Figure 2. (a) Small scale map showing the regional context of station BK.BRK (Berkeley, CA, US). Blue circular shade denotes an area within 2 km of the station. The human activity induced seismic waves that are detected by the stations are mostly generated within the blue shaded area. **(b)** Large scale map showing the area near station BK.BRK . **(c)** Displacement RMS of BK.BRK station from Dec 1, 2019 to Apr 26, 2020. Thin black curves show the displacement RMS of the 30 minute-long sliding window, and thick red curves show daily median displacement RMS amplitudes.

Figure 3. Locations of 23 seismic stations investigated in Southern California. Red pins denote the 5 stations that record a drop in human activity after the California shelter-in-place order. Black pins denote the 14 stations that are capable of reflecting human activity variation but did not record a drop in human activity after the California shelter-in-place order. Green pins denote the 4 stations appear not capable of reflecting human activity variation. The displacement RMS time-series of the 19 stations that are capable of reflecting human activity variation are shown in Figure 4. The displacement RMS time-series of the 4 stations that do not reflect human activity variation are shown in Figure S4.

Figure 4. (a) Scaled daily median displacement RMS time series of the 19 stations that show the capability of detecting human activity change (black and red pins in Figure 4). All 19 time series are plotted in black. Green horizontal dashed line denotes the Christmas/New Year break level, and Orange horizontal dashed line denotes the normal period level. Vertical purple line denotes the day when California issued a state-wide "shelter-in-place" order. **(b)** Same as Figure 4a, except that the 5 stations that show an amplitude drop after the shelter-in-place order are instead plotted in red while the other 14 stations that do not show drop remain plotted in black.

Figure 5. (a) Map showing the area near station LD.CPNY (Central Park, New York City, NY, United States). Blue circular shade denotes an area within 2km range of the station. The human activity induced seismic waves that are detected by the stations are mostly generated with the shaded area. **(b)** Map showing the area near station BC.UABX (downtown Mexicali, Baja California, Mexico). Blue circular shaded area as above. **(c)** daily median displacement RMS time series of BK.BRK (upper panel), LD.CPNY (middle panel) and BC.UABX (lower panel) from Dec 1 to Apr 26. In each sub panel, blue curves show the trends from Dec-2019 to Apr-2020 and gray curves show the trends from Dec-2018 to Apr-2019 for comparison. Vertical lines of different colors (numbered in a chronological order) denote the dates when a potential human-activity-related restriction was issued, such as "school close order" or "shelter-in-place order".

Figure 6. (a) The red solid line denotes the mean of the 5 scaled daily median displacement RMS time series that record a drop after the shelter-in-place order. The black solid line denotes the mean of the 14 scaled daily median displacement RMS time series that did not record a drop after the shelter-in-place order. The blue dashed line

809 denotes the Apple mobility "driving index" of Los Angeles City. **(b)** The scaled shelter-in-
810 place noise level against the absolute non-holiday noise level for the 19 stations that show
811 anthropogenic noise characteristics. **(c)** The average power of the seismic noise PDF of
812 the 23 surveyed stations. Red lines are the 5 stations that record a drop in anthropogenic
813 noise after shelter-in-place order. Black lines are the 14 stations that did not record a drop
814 in anthropogenic noise after shelter-in-place order. Green lines are the 4 stations that did
815 not show anthropogenic noise characteristics. Yellow and blue dashed lines denote the
816 New High Noise Model (NHNM) and the New Low Noise Model (NLNM) in Peterson
817 (1993), respectively.

818 **Figure 7.** (a) and (b): Location of CI.MSJ, CI.RVR, CI.RSS and AM.R2FCF on google
819 map. The orientation of a gray and red lines centered at a station denotes the direction
820 ϕ_m and the length of line represents the normalize amplitude I_m. Gray thin lines show the
821 ϕ_m of 1469 segments within the study period and the red thick line show the mode of
822 direction ϕ_m. (c)-(e) Histogram of direction ϕ_m of station CI.MSJ, CI.RVR, and CI.RSS,
823 respectively (f) The cross-correlation function between CI.RSS and AM.R2FCF. The gray
824 lines denote the day-correlation function of each 14 day and the purple line denotes the
825 stack correlation function. Pulse on the negative time axis means signal propagating from
826 CI.RSS to AM.R2FCF.

827 **Figure 8. (a)** Comparisons between the average daily precipitation in Southern California
828 and the 14 daily displacement RMS time series that do not show a significant drop in
829 amplitude after the “shelter-in-place” order. Gray thin curves are the individual time series
830 of the 14 stations. Purple curves are the mean variation of the 19 individual time series.
831 Green curves are the average daily precipitation time series over the 14 areas that are

832 covered by the National Weather Service (NWS) Office in Los Angeles/Oxnard and in
833 San Diego. **(b)** Comparisons between the average daily precipitation in Southern
834 California and the 5 daily displacement RMS time series that show a significant drop in
835 amplitude after the shelter-in-place order. Gray thin curves are the individual time series
836 of the 5 stations. Purple curves are the mean variation of the 5 individual time series.
837 Green curves are the average daily precipitation time series in Southern California (same
838 as Figure 8a).

839 **Figure 9. (a)** Map showing the area near station CI.MSJ and CI.RSS (Hemet area and
840 Riverside area, California, United States). Blue circular shading denotes an area within
841 2km range of the station. The human activity induced seismic waves that are detected by
842 the stations are mostly generated within the shaded area. **(b)** daily median displacement
843 RMS time series of CI.MSJ (upper panel) and CI.RSS (lower panel) from Dec 1 to Apr
844 26. In each sub panel, blue curves show the trends from Dec-2019 to Apr-2020 and gray
845 curves show the trends from Dec-2018 to Apr-2019. The purple vertical dash lines denote
846 the dates when a “school close order” was implemented.

847 **Figure 10.** Comparisons between the ground vibration amplitude and the Apple mobility
848 "driving index". From top to bottom are BK.BRK, LD.CPNY and BC.UABX, respectively.
849 In each sub panel, blue curves show the trends of daily median displacement RMS from
850 Dec-2019 to Apr-2020, and orange curves show the Apple mobility "driving index" trends
851 in the same period.

Figures

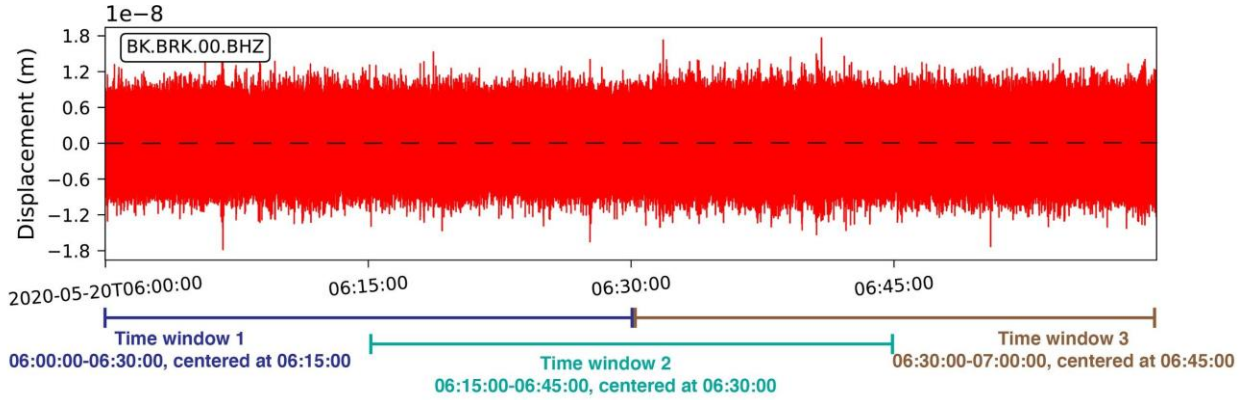

Figure 1. An example of a seismic record demonstrating how the sliding time-windows are used to compute displacement root mean square (RMS) time series. The seismogram in red is 1 hour of a vertical component seismogram (BHZ) at station BK.BRK filtered at 4-14 Hz (from 2020-05-20, 6am to 7am, local time). The blue, cyan, and brown horizontal lines below the plot denote the three, 30 minutes long overlapping sliding time windows within this one hour.

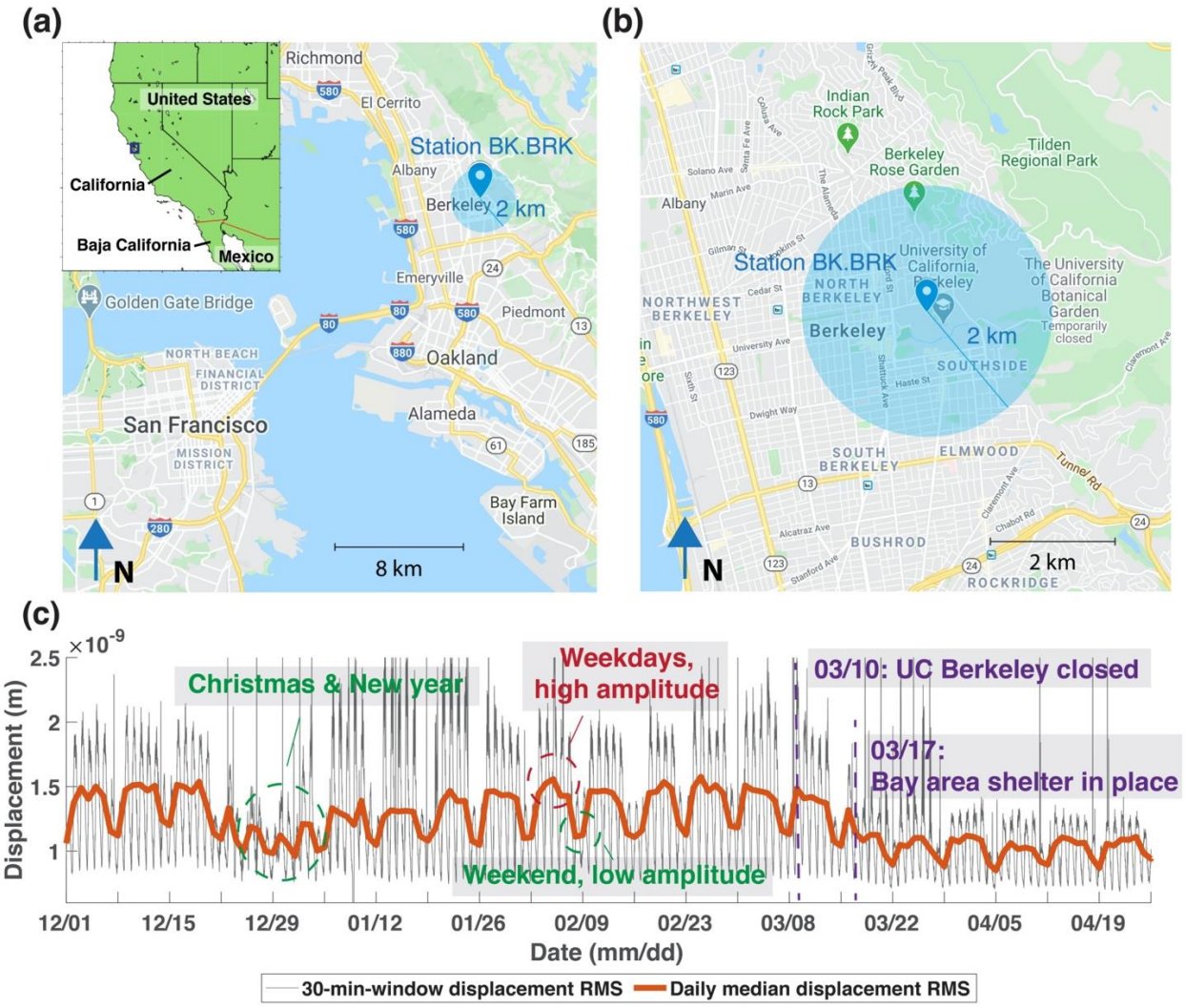

Figure 2. (a) Small scale map showing the regional context of station BK.BRK (Berkeley, CA, US). Blue circular shade denotes an area within 2 km of the station. The human activity induced seismic waves that are detected by the stations are mostly generated within the blue shaded area. **(b)** Large scale map showing the area near station BK.BRK . **(c)** Displacement RMS of BK.BRK station from Dec 1, 2019 to Apr 26, 2020. Thin black curves show the displacement RMS of the 30 minute-long sliding window, and thick red curves show daily median displacement RMS amplitudes.

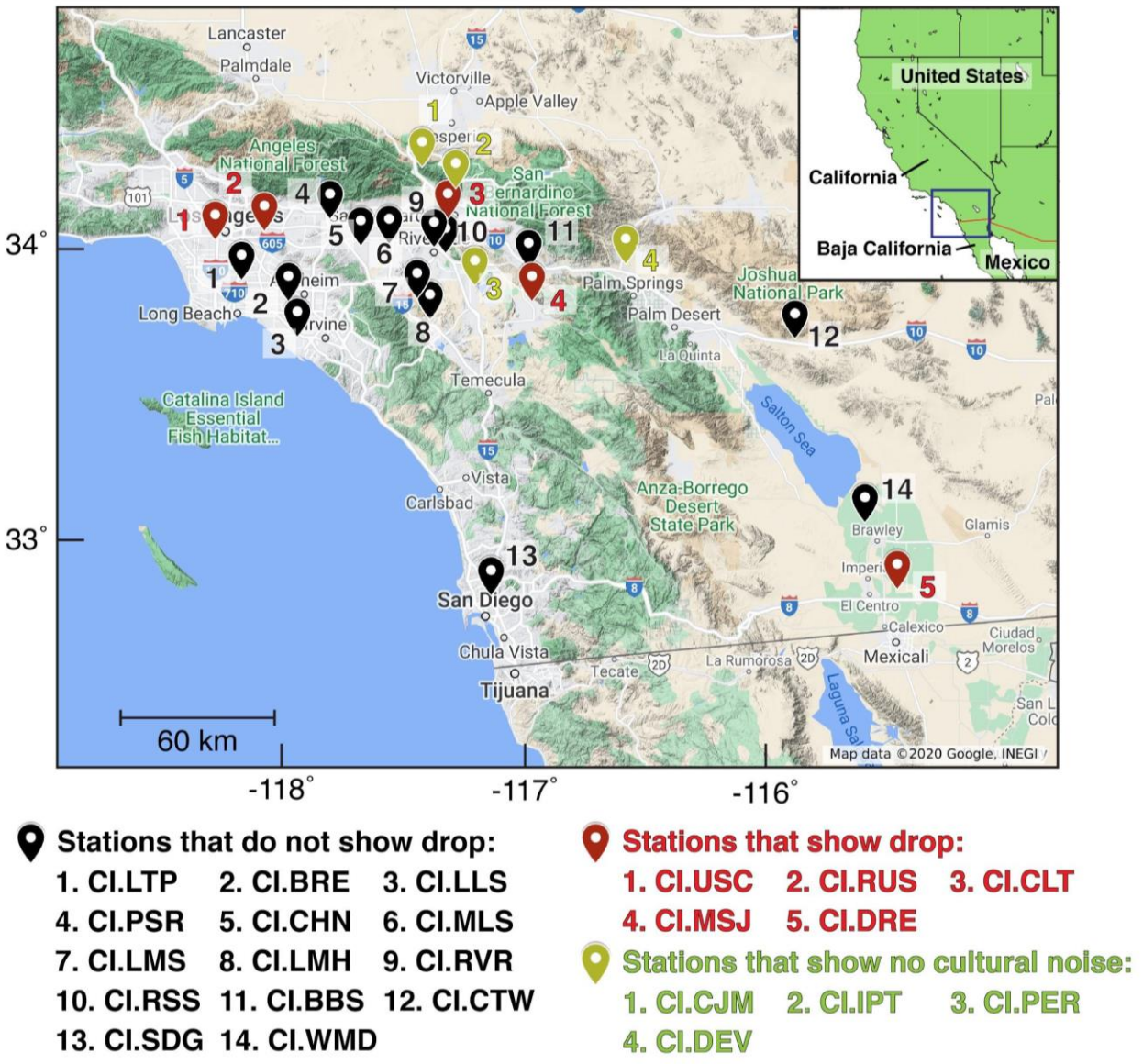

Figure 3. Locations of 23 seismic stations investigated in Southern California. Red pins denote the 5 stations that record a drop in human activity after the California shelter-in-place order. Black pins denote the 14 stations that are capable of reflecting human activity variation but did not record a drop in human activity after the California shelter-in-place order. Green pins denote the 4 stations appear not capable of reflecting human activity variation. The displacement RMS time-series of the 19 stations that are capable of

875 reflecting human activity variation are shown in Figure 4. The displacement RMS time-
876 series of the 4 stations that do not reflect human activity variation are shown in Figure S4.

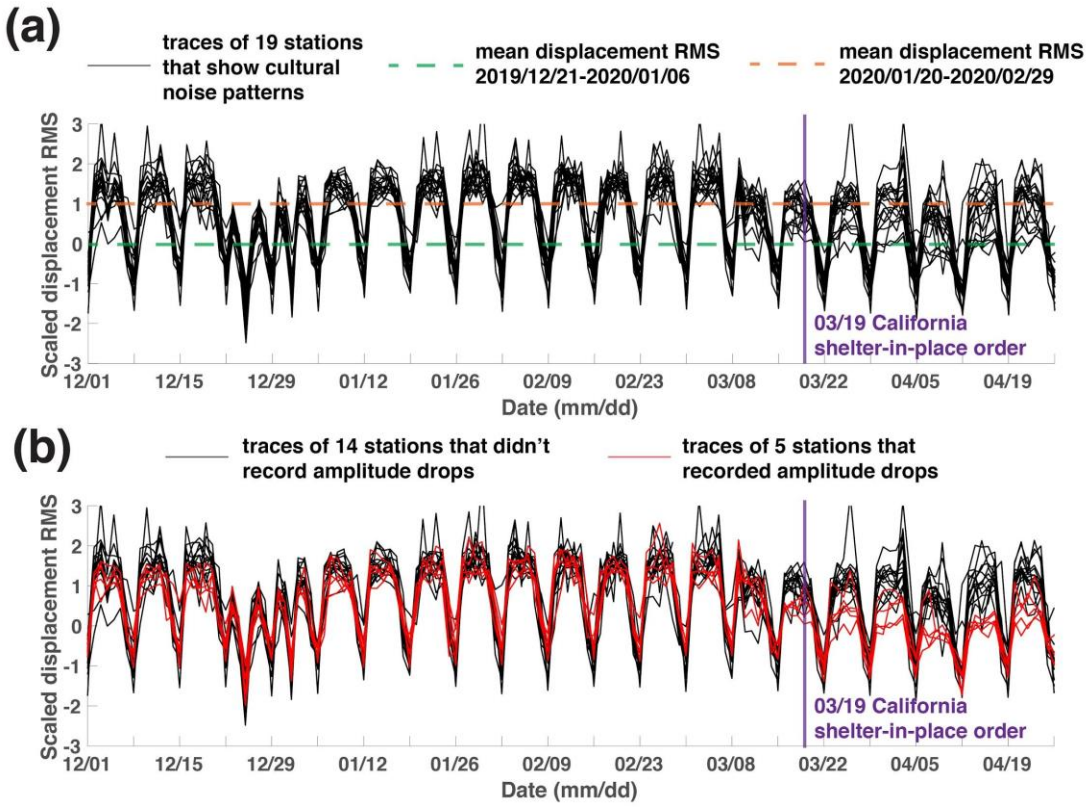

877

878 **Figure 4. (a)** Scaled daily median displacement RMS time series of the 19 stations that
879 show the capability of detecting human activity change (black and red pins in Figure 4).
880 All 19 time series are plotted in black. Green horizontal dashed line denotes the
881 Christmas/New Year break level, and Orange horizontal dashed line denotes the normal
882 period level. Vertical purple line denotes the day when California issued a state-wide
883 shelter-in-place order. **(b)** Same as Figure 4a, except that the 5 stations that show an
884 amplitude drop after the shelter-in-place order are instead plotted in red while the other
885 14 stations that do not show drop remain plotted in black.

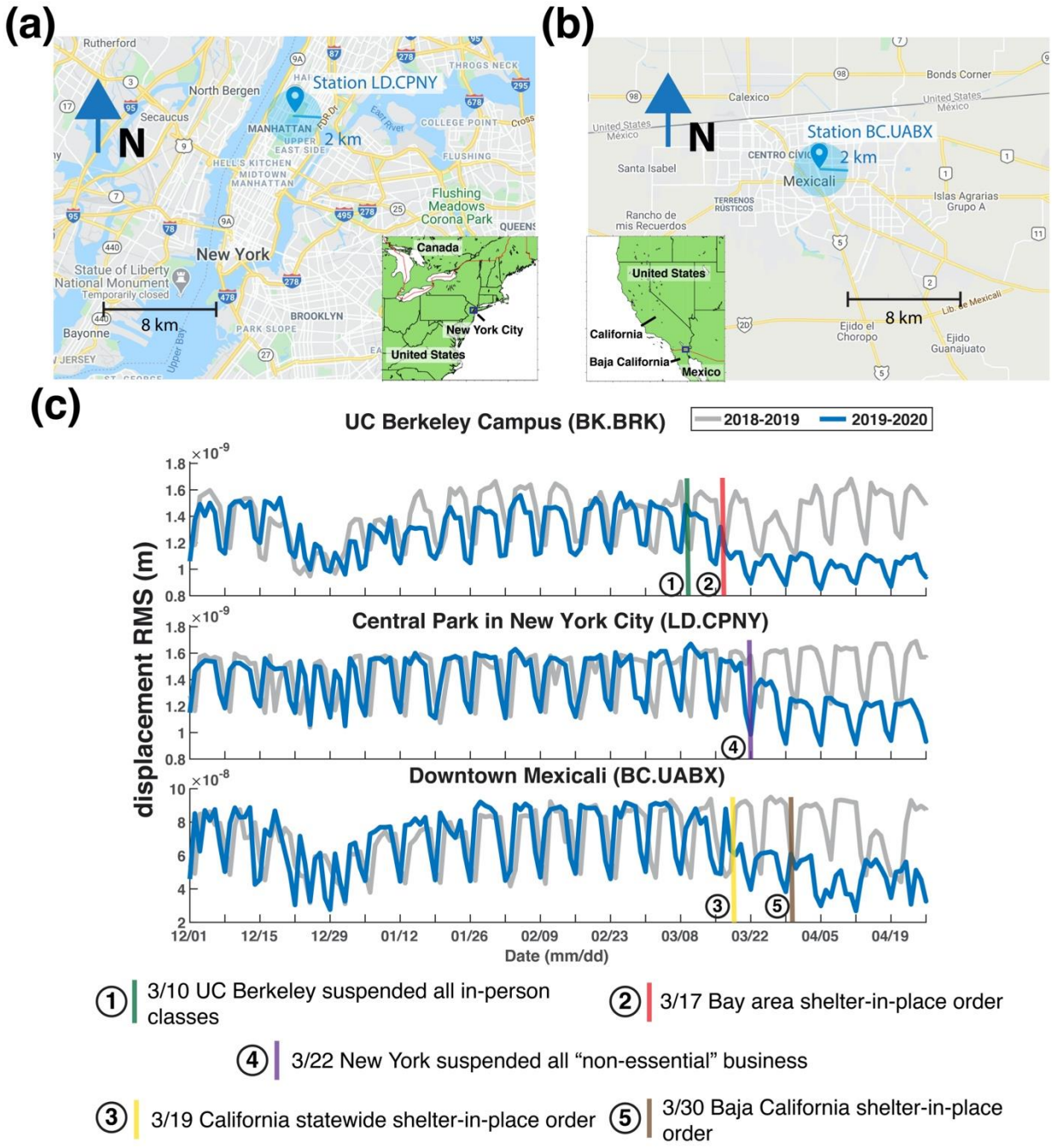

Figure 5. (a) Map showing the area near station LD.CPNY (Central Park, New York City, NY, United States). Blue circular shade denotes an area within 2km range of the station. The human activity induced seismic waves that are detected by the stations are mostly generated with the shaded area. **(b)** Map showing the area near station BC.UABX (downtown Mexicali, Baja California, Mexico). Blue circular shaded area as above. **(c)**

892 daily median displacement RMS time series of BK.BRK (upper panel), LD.CPNY (middle
893 panel) and BC.UABX (lower panel) from Dec 1 to Apr 26. In each sub panel, blue curves
894 show the trends from Dec-2019 to Apr-2020 and gray curves show the trends from Dec-
895 2018 to Apr-2019 for comparison. Vertical lines of different colors (numbered in a
896 chronological order) denote the dates when a potential human-activity-related restriction
897 was issued, such as “school close order” or “shelter-in-place order”.

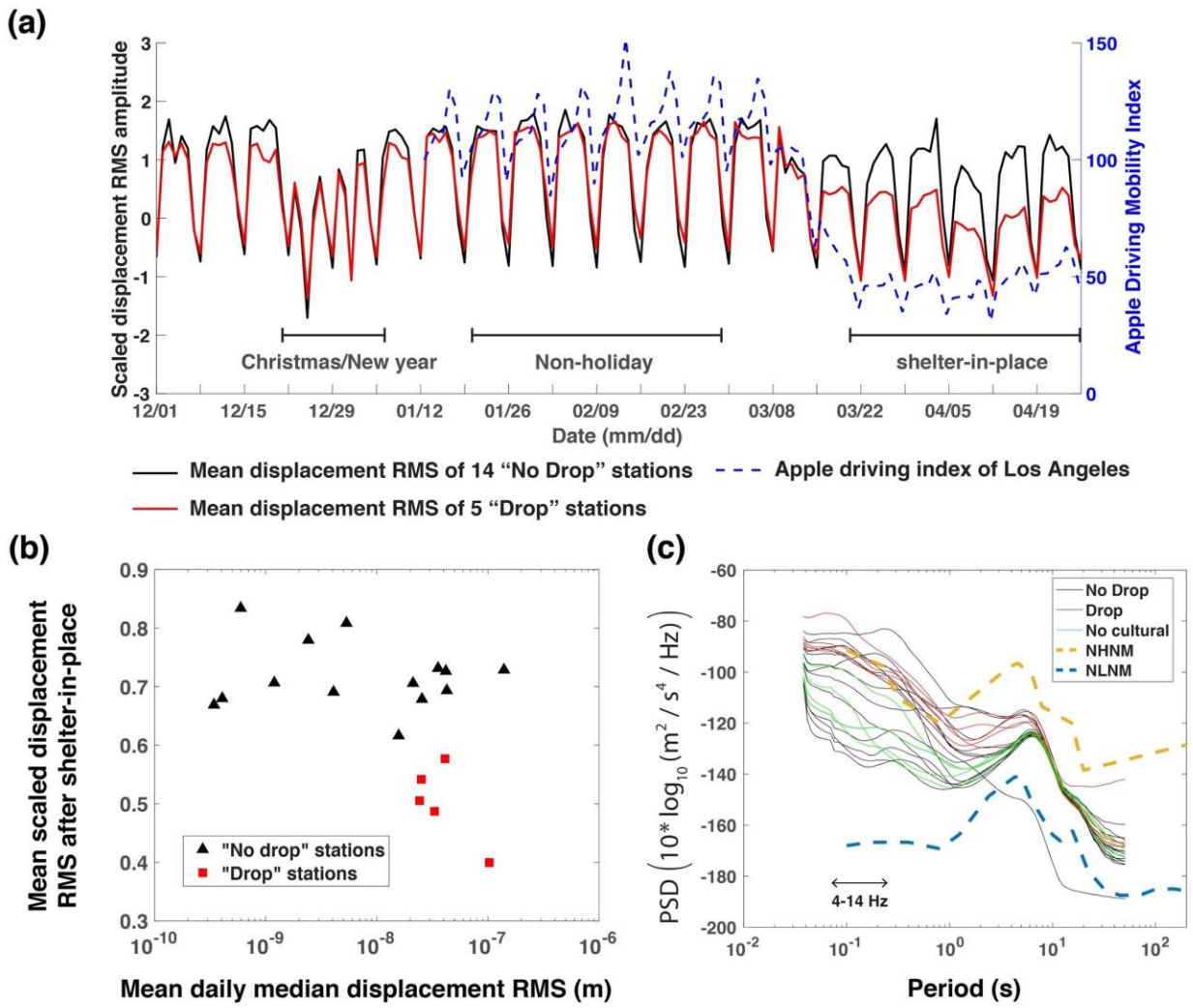

898

899 **Figure 6. (a)** The red solid line denotes the mean of the 5 scaled daily median
900 displacement RMS time series that record a drop after the shelter-in-place order. The
901 black solid line denotes the mean of the 14 scaled daily median displacement RMS time
902 series that did not record a drop after the shelter-in-place order. The blue dashed line
903 denotes the Apple mobility "driving index" of Los Angeles City. **(b)** The scaled shelter-in-
904 place noise level against the absolute non-holiday noise level for the 19 stations that show
905 anthropogenic noise characteristics. **(c)** The average power of the seismic noise PDF of
906 the 23 surveyed stations. Red lines are the 5 stations that record a drop in anthropogenic

907 noise after shelter-in-place order. Black lines are the 14 stations that did not record a drop
908 in anthropogenic noise after shelter-in-place order. Green lines are the 4 stations that did
909 not show anthropogenic noise characteristics. Yellow and blue dashed lines denote the
910 New High Noise Model (NHNM) and the New Low Noise Model (NLNM) in Peterson
911 (1993), respectively.

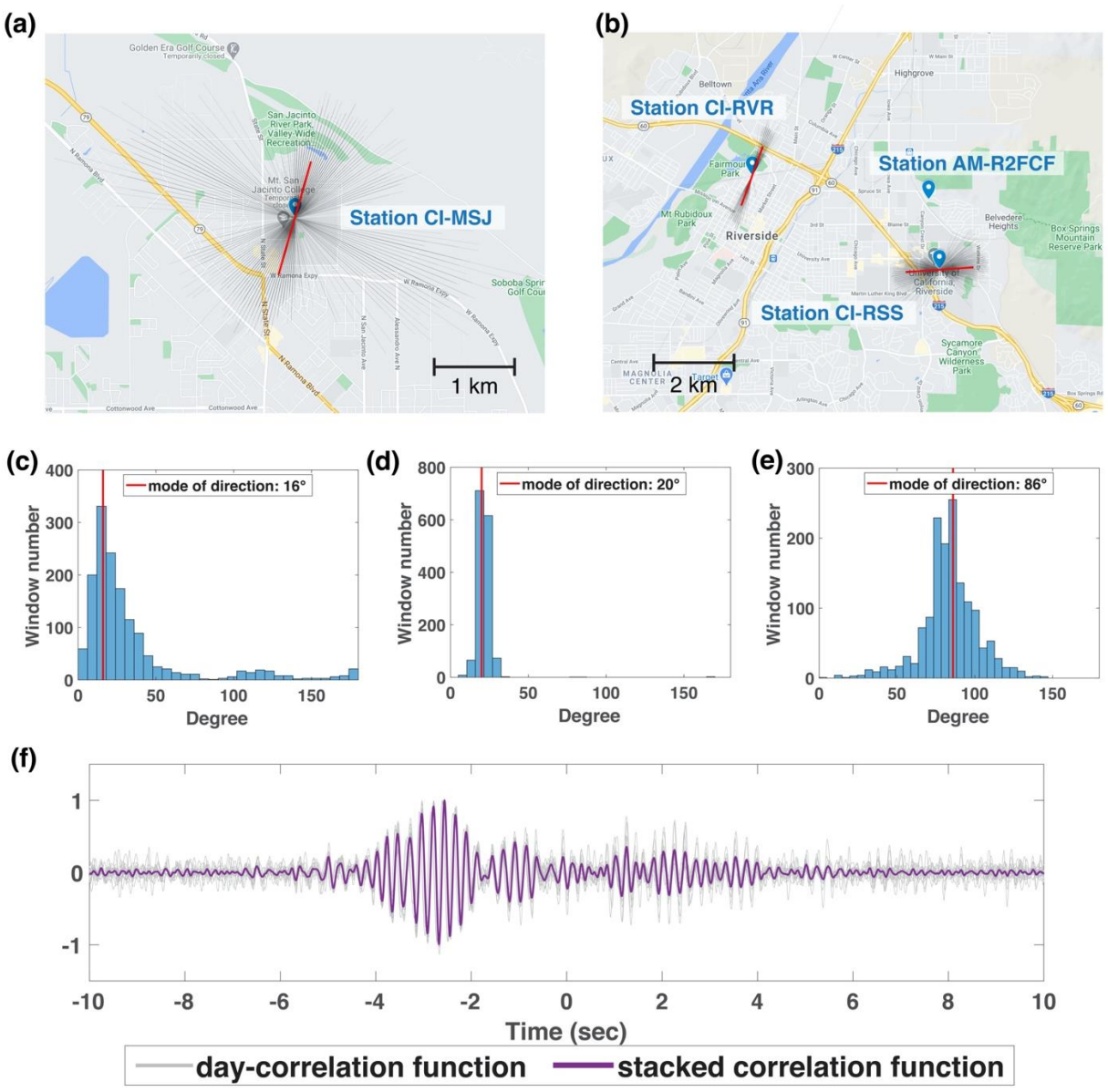

912

913 **Figure 7.** (a) and (b): Location of CI.MSJ, CI.RVR, CI.RSS and AM.R2FCF on google
914 map. The orientation of a gray and red lines centered at a station denotes the direction
915 ϕ_m and the length of line represents the normalize amplitude I_m. Gray thin lines show the
916 ϕ_m of 1469 segments within the study period and the red thick line show the mode of
917 direction ϕ_m. (c)-(e) Histogram of direction ϕ_m of station CI.MSJ, CI.RVR, and CI.RSS,
918 respectively (f) The cross-correlation function between CI.RSS and AM.R2FCF. The gray

lines denote the day-correlation function of each 14 day and the purple line denotes the stack correlation function. Pulse on the negative time axis means signal propagating from CI.RSS to AM.R2FCF.

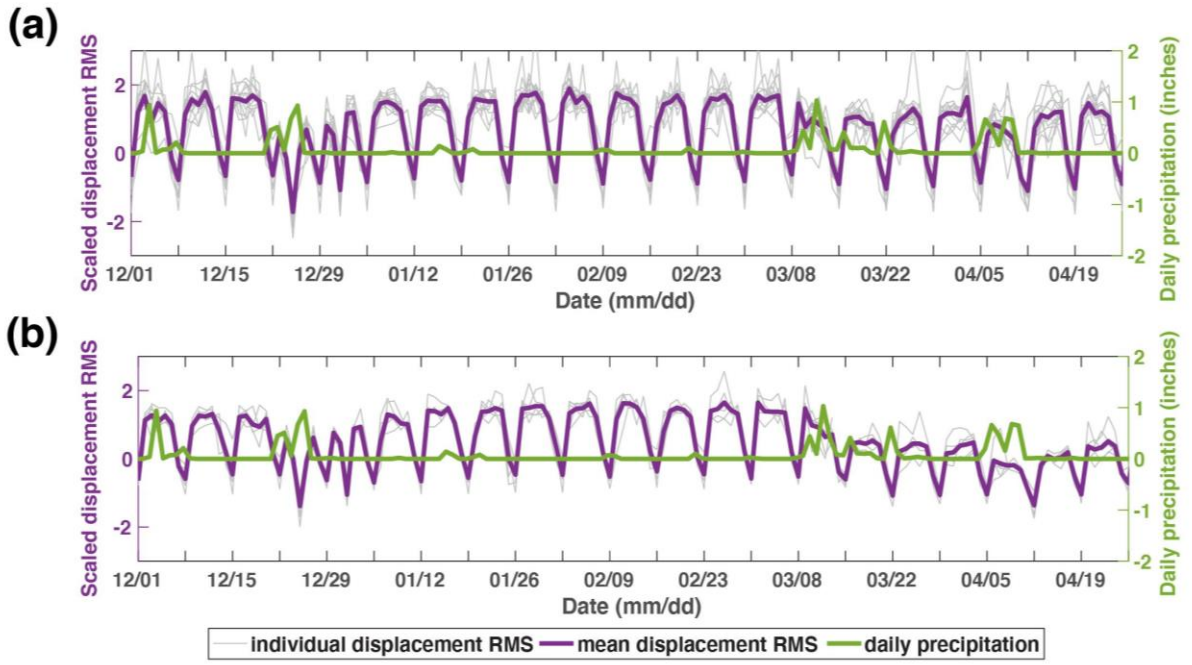

Figure 8. (a) Comparisons between the average daily precipitation in Southern California and the 14 daily displacement RMS time series that do not show a significant drop in amplitude after the shelter-in-place order. Gray thin curves are the individual time series of the 14 stations. Purple curves are the mean variation of the 19 individual time series. Green curves are the average daily precipitation time series over the 14 areas that are covered by the National Weather Service (NWS) Office in Los Angeles/Oxnard and in San Diego. **(b)** Comparisons between the average daily precipitation in Southern California and the 5 daily displacement RMS time series that show a significant drop in amplitude after the shelter-in-place order. Gray thin curves are the individual time series of the 5 stations. Purple curves are the mean variation of the 5 individual time series. Green curves are the average daily precipitation time series in Southern California (same as Figure 8a).

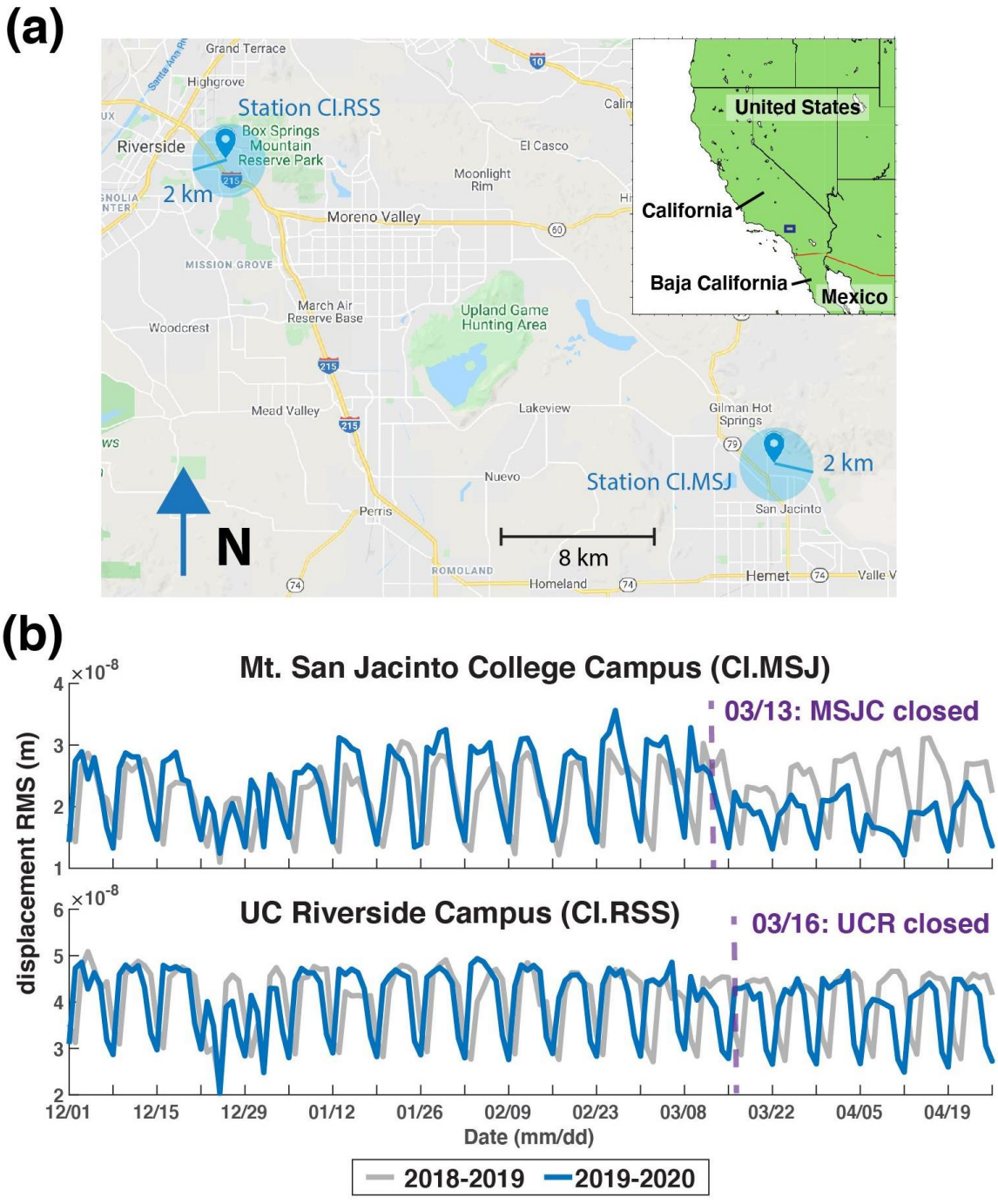

935

936 **Figure 9. (a)** Map showing the area near station CI.MSJ and CI.RSS (Hemet area and
937 Riverside area, California, United States). Blue circular shading denotes an area within
938 2km range of the station. The human activity induced seismic waves that are detected by
939 the stations are mostly generated within the shaded area. **(b)** daily median displacement

940 RMS time series of CI.MSJ (upper panel) and CI.RSS (lower panel) from Dec 1 to Apr
941 26. In each sub panel, blue curves show the trends from Dec-2019 to Apr-2020 and gray
942 curves show the trends from Dec-2018 to Apr-2019. The purple vertical dash lines denote
943 the dates when a “school close order” was implemented.

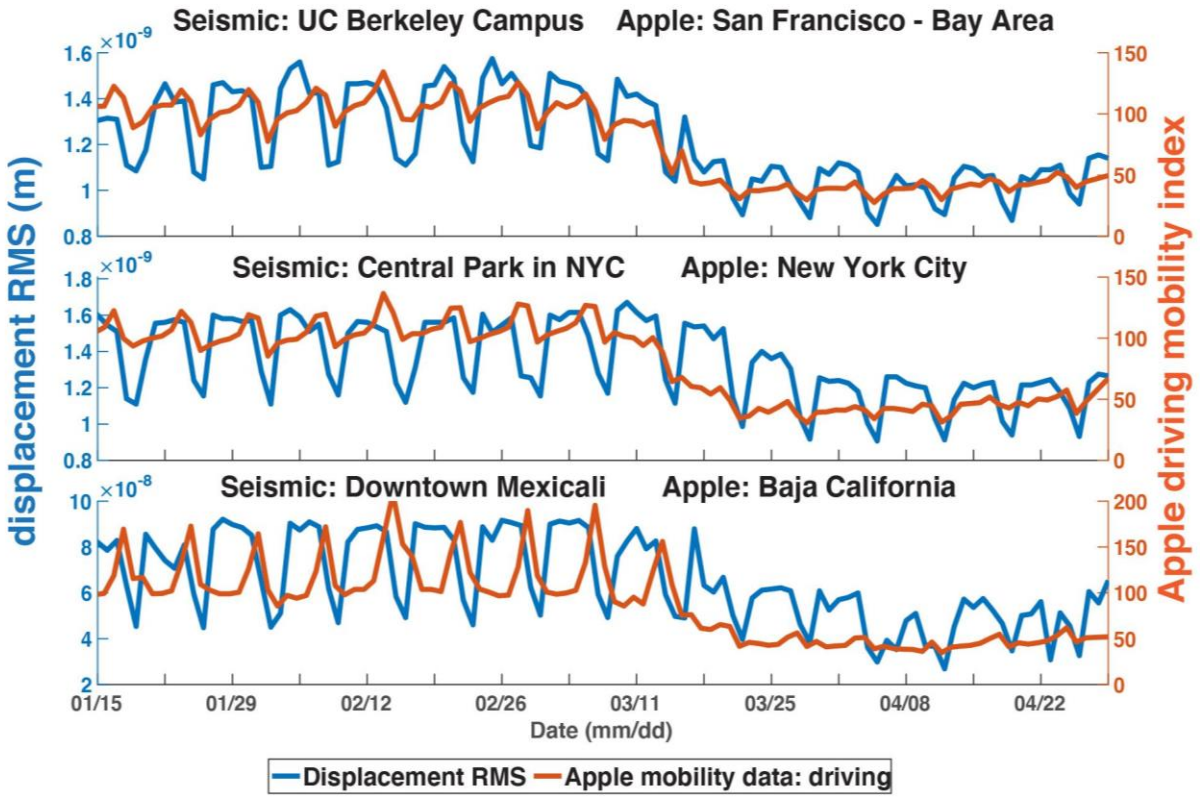

Figure 10. Comparisons between the ground vibration amplitude and the Apple mobility "driving index". From top to bottom are BK.BRK, LD.CPNY and BC.UABX, respectively. In each sub panel, blue curves show the trends of daily median displacement RMS from Dec-2019 to Apr-2020, and orange curves show the Apple mobility "driving index" trends in the same period.